Heliyon 10 (2024) e27686

Contents lists available at ScienceDirect

Heliyon

journal homepage: www.cell.com/heliyon

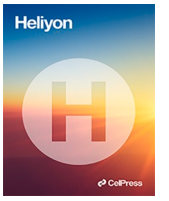

Research article

Translating microcalcification biomarker information into the laboratory: A preliminary assessment utilizing core biopsies obtained from sites of mammographic calcification

Iain D. Lyburn [a], Robert Scott [b], Eleanor Cornford [a], Pascaline Bouzy [c], Nicholas Stone [c], Charlene Greenwood [d], Ihsanne Bouybayoune [e], Sarah E. Pinder [e], Keith Rogers [b,*]

[a] Gloucestershire Hospitals NHS Foundation Trust, Cheltenham, United Kingdom
[b] Cranfield Forensic Institute, Cranfield University, Swindon, United Kingdom
[c] School of Physics and Astronomy, University of Exeter, Exeter, United Kingdom
[d] School of Chemical and Physical Sciences, Keele University, Staffordshire, United Kingdom
[e] School of Cancer and Pharmaceutical Sciences, King's College London, London, United Kingdom

ARTICLE INFO

Keywords:
Microcalcification
X-ray scatter
Crystallography
Biomarker

ABSTRACT

Rationale and objectives: The potential of breast microcalcification chemistry to provide clinically valuable intelligence is being increasingly studied. However, acquisition of crystallographic details has, to date, been limited to high brightness, synchrotron radiation sources. This study, for the first time, evaluates a laboratory-based system that interrogates histological sections containing microcalcifications. The principal objective was to determine the measurement precision of the laboratory system and assess whether this was sufficient to provide potentially clinical valuable information.

Materials and methods: Sections from 5 histological specimens from breast core biopsies obtained to evaluate mammographic calcification were examined using a synchrotron source and a laboratory-based instrument. The samples were chosen to represent a significant proportion of the known breast tissue, mineralogical landscape. Data were subsequently analysed using conventional methods and microcalcification characteristics such as crystallographic phase, chemical deviation from ideal stoichiometry and microstructure were determined.

Results: The crystallographic phase of each microcalcification (e.g., hydroxyapatite, whitlockite) was easily determined from the laboratory derived data even when a mixed phase was apparent. Lattice parameter values from the laboratory experiments agreed well with the corresponding synchrotron values and, critically, were determined to precisions that were significantly greater than required for potential clinical exploitation.

Conclusion: It has been shown that crystallographic characteristics of microcalcifications can be determined in the laboratory with sufficient precision to have potential clinical value. The work will thus enable exploitation acceleration of these latent microcalcification features as current dependence upon access to limited synchrotron resources is minimized.

* Corresponding author.
E-mail address: k.d.rogers@cranfield.ac.uk (K. Rogers).

https://doi.org/10.1016/j.heliyon.2024.e27686
Received 3 June 2023; Received in revised form 4 March 2024; Accepted 5 March 2024
Available online 11 March 2024

1. Introduction

The morphology and distribution of mammographic calcifications can provide vital diagnostic and prognostic information, augmented recently using artificial intelligence (A.I.) [1–3]. However, details of their precise chemical nature and their formation mechanisms remain unclear and therefore their full potential as diagnostic biomarkers cannot be fulfilled. The mechanisms by which calcifications form can range from active cellular processes to unregulated deposition on necrotic cellular debris [4]. Further debate concerns the role of osteo-proteins (e.g., osteopontins) which have been implicated in formation of breast microcalcifications [5] although the lack of an affiliation with collagen confounds this potential pathway. *In-vitro* studies show that differences in cellular microenvironment can change the mineralisation pathway by which calcifications form [6].

There has been a significant increase in the number of studies examining the minerology of microcalcifications in breast as well as other tissues, and these have been accelerated by the evidenced premise that a diagnostic advantage may be derived from microcalcification chemistry [7,8] For instance, it is widely accepted that calcium oxalate calcifications result from benign processes of formation, whereas apatites can form in both benign conditions or malignant tumours. More recently, studies have focussed on the crystallography of apatite calcifications, whose crystal lattice has a remarkable capacity for ionic substitution. The crystal structure therefore retains information on the elemental microenvironment of the tissue in which they formed [9]. For example, reduced substitution of CO_3^{2-} for lattice PO_4^{3-} and OH^- is associated with increased malignancy [10]. These ionic substitutions distort the crystal lattice and inhibit crystal growth, thus the degree of substitution can be inferred from measurements of the crystal lattice parameters (a set of numerical values that define the size and morphology of the atomic lattice structure).

Several recent research programmes provide a unique insight into the relationships between breast pathology and the crystallographic attributes of microcalcifications. These have successfully employed the X-ray scattering signatures of microcalcifications to reveal unique crystallographic features such as phase, lattice parameters and microstructure. Of note are two major, retrospective studies (CRUK's 'Precision' and MRC's 'Capture') that are characterising microcalcifications in situ (within histological sections for the first time) thus retaining the context of the surrounding tissue. Furthermore, x-ray diffraction can provide unequivocal identification of the crystallographic phases present in a calcification, unlike elemental studies in which phases can easily be mis-identified [11].

However, both studies have been dependent upon the use of synchrotron radiation (SR) X-ray sources only available at National centers (e.g., the Diamond Light Source in the U.K.). Although this has been appropriate as a research tool to investigate the relationship between crystallographic parameters and pathology in microcalcifications, access to these facilities is not practical as a routine clinical tool thus there is a technological gap in data acquisition solutions Moreover, high-resolution imaging data from micron sized X-ray beams using SR is useful for basic research into calcification pathogenesis, but is not necessary if only the average chemical characteristics of individual microcalcifications are required.

Thus, the primary objective of this brief preliminary study was to assess, for the first time, the ability of conventional laboratory-based instruments to provide microcalcification chemistry features at the precision required to have clinical value. Laboratory based systems have not previously been used to examine calcifications retained within 5 μm histological sections. The subsequent data was examined both qualitatively and quantitively and a direct laboratory SR comparison undertaken.

2. Material and methods

Example cases were selected from the Gloucestershire Hospitals NHS Foundation Trust diagnostic archive and from King's Health Partners Cancer Biobank. The cases were selected from a large sample set associated with the Capture study and details are summarized within Table 1. The specific microcalcifications examined were representative of the major groups found within the mineralogical landscape of breast tissues; calcium hydroxyapatite (HAP), whitlockite and an apatite-whitlockite combination. 5 μm thick Formalin-Fixed Paraffin-Embedded (FFPE) unstained sections were mounted onto 12.5 μm thick polyolefin substrates stretched over 38 mm diameter aluminium rings and held in place with flexible rings. Each section was given a unique code as G001, G010, G030, G156 and G145.

The SR X-ray diffraction data was collected using 12 keV photons on the I18 beamline at Diamond Light Source, Didcot UK, and the corresponding laboratory diffraction data was collected using a Bruker D8 Discover diffractometer and 8.05 keV photons. The measurement probes for the SR and laboratory measurements respectively were a 5 μm × 5 μm square and a 500 μm diameter disk. Acquisition times for the SR data collections were 15 s and for the laboratory collections, 12 h. In both experiments, sections were mounted perpendicular to the X-ray beam and calcifications were identified using a microscope mounted at 45° to the sample stage. In contrast to the laboratory-based experiment, where a complete microcalcification was examined in a single acquisition (thus averaging the diffraction signal), the SR data was acquired from a volume significantly less than that of the calcification as indicated by the

Table 1
Pathology opinion and BI-RADS classification for the selected cases.

Specimen	Pathology Opinion	BI-RADS distribution	BI-RADS morphology
G001	B3, lesion of uncertain malignant potential	segmental	Coarse heterogeneous
G010	B2, benign	grouped	Coarse or popcorn-like
G030	B5b, grade 3 invasive cancer	grouped	Amorphous
G145	B5a, high grade ductal carcinoma in situ	segmental	Fine pleomorphic
G156	B5a, high grade ductal carcinoma in situ	grouped	Coarse heterogeneous

measurement dimensions.

Data reduction, from 2D scatter distributions to calibrated 1D 'diffractograms', was undertaken through conventional integration and calibration steps using Bruker GADDS software. The diffractograms were parameterized using the analytical software Topas 6.0 (Bruker AXS) and this provided values for the principal crystallographic characteristics that are correlated to tissue type. Interplaner spacings (d) were calculated using Bragg's Law, $d = \lambda/(2\sin\theta)$ where λ is the interrogating X-ray wavelength and θ is the scatter angle. Lattice parameters were calculated using a whole pattern fit of hydroxyapatite and whitlockite, with a Stephens model to adjust for the marked anisotropy observed in these specimens. Individual peak widths were extracted from a peaks-fit using positions calculated from the previously derived lattice parameters. Estimated standard deviations (precision estimates) were calculated using conventional, non-linear least squares methods from singular value decomposition of the whole pattern fit [12]. This provides the basis for comparing values but does not enable frequentist inference, hypothesis testing.

IRB ethics approval was provided through National Health Service HRA/HCRW Ethics Approval (REC reference 20/NW/0057), granted in February 2020. Tissue sections were allocated a pseudonymised study number.

3. Results

Fig. 1 (a – d) exemplifies the spatial scale relationship between the mammographic and histological appearance of microcalcifications and the scale of a typical individual calcification examined within this work illustrated by an electron micrograph. For this example, the calcification width was approximately 50 μm.

Raw X-ray scatter data is presented in the form of conventional 1D diffractograms (intensity as a function of scatter angle) where scattering distributions are characterized by maxima within the X-ray intensities at atomic spacings ('d-spacings'). Such signatures are unique for crystallographic phase and the analytical study of diffractograms reveals details of atomic spatial distributions and distortions from the ideal (energy minimized) structures. Fig. 2 shows unadulterated diffractograms arising from calcifications measured using laboratory (upper trio) and SR sources (lower trio). The plots are arranged to compare the data from different microcalcifications using both sources. The laboratory data are typical of those corresponding to biologically derived hydroxyapatite in a nano-crystalline form, although the signal to noise ratio (S/N) for the SR data is significantly greater than that from the laboratory source. Fig. 3 illustrates the signals from other microcalcifications that clearly show the reasonable correspondence between intensity maxima positions from laboratory and SR sources. This indicates that the specific mineral phase can be unequivocally determined from the

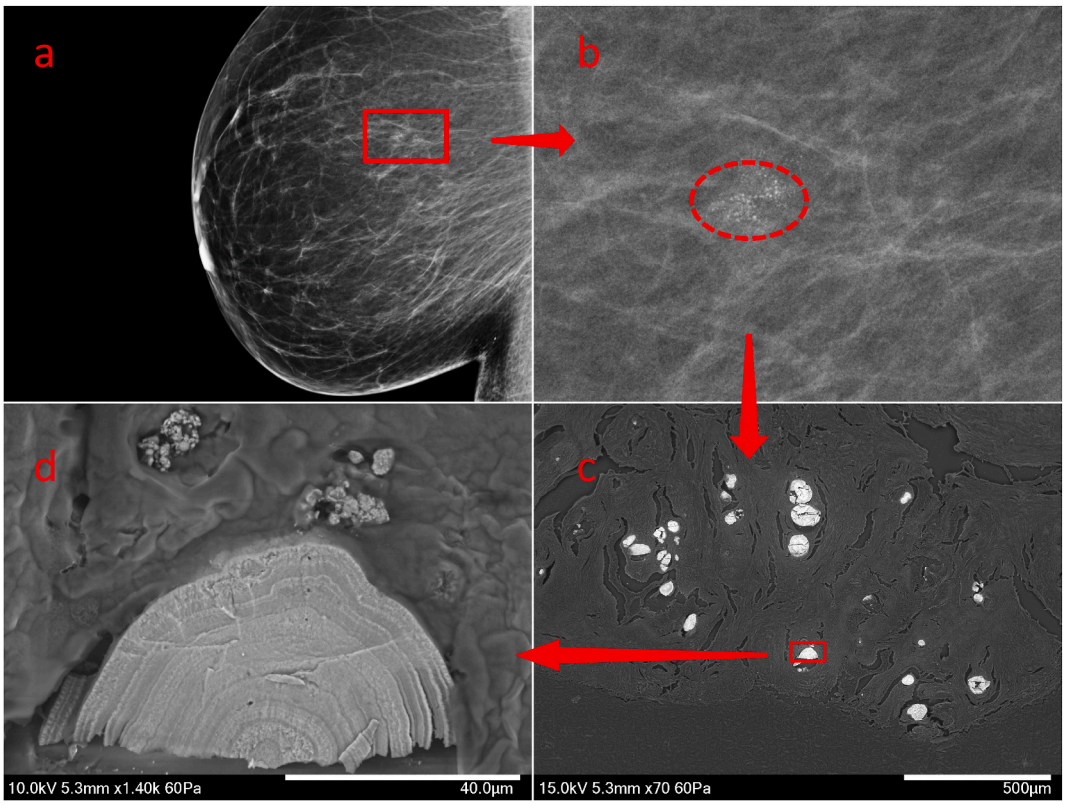

Fig. 1. Microcalcification appearance at increasing magnification from mammogram (a), magnification-view mammogram (b), low magnification (x70) SEM image (c), higher magnification (x1400) SEM image (d). The area of any single SR data point was approximately 10% of that of the electron micrograph scale in image (d), and the corresponding laboratory data point area was covered the whole calcification illustrated.

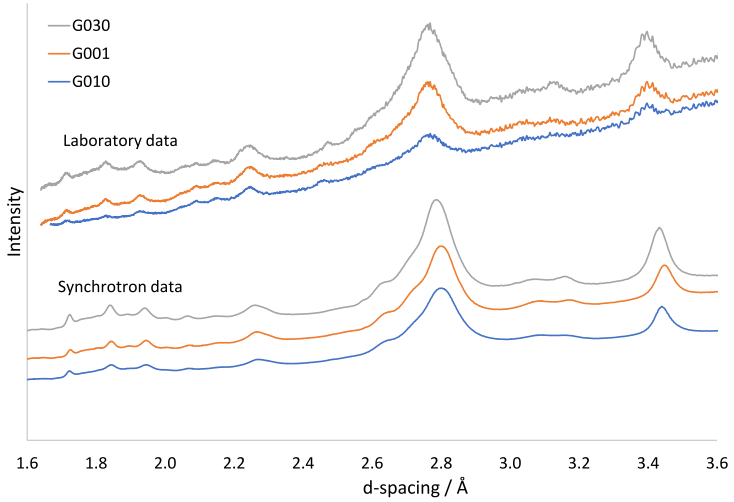

Fig. 2. X-ray scatter distributions from hydroxyapatite microcalcifications collected using the laboratory-based system; (a) G030, (b) G001, (c) G010 and the corresponding scatter data collected using synchrotron radiation; (d) G030, (e) G001 and (f) G010.

Fig. 3. X-ray scatter distributions from microcalcifications that were compositionally distinct from pure hydroxyapatite. Measured using the laboratory-based system are (a) G145 showing data consistent with pure whitlockite, (b) G156 showing data consistent with a mixture of whitlockite and apatite. The corresponding data measured using synchrotron radiation are (c) G145 (pure whitlockite) and, (d) G156 (a whitlockite, apatite mix).

laboratory data, the upper diffractogram corresponds to exclusively whitlockite and the lower is a mix of hydroxyapatite and whitlockite. Note that the hydroxyapatite intensity maxima are, in general, broader than those of the whitlockite in the laboratory data indicating significantly different microstructures for the two phases. This is consistent with the SR data.

To quantitively assess parameter precision, data were parameterised to produce crystallographic lattice parameters for hydroxyapatite and whitlockite phases. These are presented in Table 2 for both laboratory and SR sources.

In all cases except G030, the HAP 'a' lattice parameter values derived from the laboratory data are within 2.5 standard deviations of the corresponding SR values and two out of four of the laboratory derived HAP 'c' values are within 2.5 standard deviations of the corresponding SR values. Except for G145 'c' lattice parameter, all the whitlockite lattice parameter values for the laboratory data are

Table 2
Values of clinically significant variables (apatite and whitlockite lattice parameters) derived from the maxima within (a) laboratory and (b) SR scatter data. Precision estimates are provided as standard deviations for each value.

	Hydroxyapatite				Hydroxyapatite			
Calcification	a/Å	σ(a)	c/Å	σ(c)	a/Å	σ(a)	c/Å	σ(c)
G001	9.421	0.0045	6.899	0.0032	9.424	0.0011	6.901	0.0007
G010	9.439	0.0060	6.912	0.0043	9.442	0.0013	6.899	0.0007
G030	9.422	0.0055	6.898	0.0040	9.443	0.0012	6.918	0.0008
G156	9.427	0.0023	6.906	0.0018	9.431	0.0009	6.902	0.0006
	Whitlockite				**Whitlockite**			
G145	10.374	0.0041	37.321	0.0140	10.368	0.0011	37.564	0.0067
G156	10.358	0.0025	37.242	0.0094	10.357	0.0008	37.245	0.0033
(a) Laboratory derived					*(b) Synchrotron derived*			

within 2.5 standard deviations of the corresponding SR data. Overall, and as expected given the S/N differences, the measurement precision associated with the SR values is significantly better than that of the laboratory data. Importantly, the average relative error for laboratory and synchrotron derived hydroxyapatite lattice parameters is 0.05% and 0.01% respectively. The average relative error for laboratory and synchrotron derived whitlockite lattice parameters is 0.03% and 0.01% respectively.

The microstructural information measured using these methods characterises the domain size and shape of the nano-crystallites and is manifest in the intensity maxima shape. Narrow, sharp peaks are indicative of a high degree of crystalline order, whereas broad peaks are indicative of small crystallite size and/or inhomogenous strain from ionic substitutions within the lattice. This can indicate the maturity of the calcification and therefore its propensity for resorption and subsequent modification of the local tissue microenvironment ionic milieu. Each intensity maximum corresponds to scattering in a different crystallographic direction, and in the case of biogenic apatites there is generally a strong direction dependence. Peak widths from the laboratory data were used to calculate the volume-weighted thickness of the coherently diffracting domains in the crystallographic direction corresponding to each peak [13]. These are plotted in Fig. 4. This is polar plot with radial distance from the origin equal to half the calculated thickness, and angle representing crystallographic direction. Ellipses were fitted to these points using a least-squares fit, weighted by the reciprocal of the coefficient of variation of the peak widths. This provides a direct semi-quantitative representation of the dimensions of the coherently diffracting domains. The anisotropy of the apatite in the calcifications can clearly be seen. Calculated size and aspect ratio are consistent with previous synchrotron measurements [14]. For reference, laboratory diffraction data from synthetic hydroxyapatite (NIST Standard Reference Material 2910b) has also been plotted. In this case, the circular shape corresponds to an equiaxed microstructure. These features can also be compared quantitatively; the three calcifications illustrated were determined to have mean domain sizes of 19.60 nm (±4 nm) and 20.6 nm (±1.1 nm) for the laboratory and SR measured data respectively.

4. Discussion

Phase composition of microcalcifications in breast tissue has previously been measured using a laboratory x-ray diffractometer in calcifications dissected from tissue [15], and using SR in calcifications within histological sections [14]. The former is time consuming and impractical for more than a small number of relatively large calcifications, which are moreover removed from the context of surrounding tissue; the latter requires access to a synchrotron, which is not readily available on demand. The data presented here are the first report of a laboratory based scattering experiment distinguishing between different crystallographic phases in microcalcifications within a 10 μm histological section, including mixtures of hydroxyapatite and whitlockite.

As indicated in the introduction, apatite lattice parameters can give some insight into the ionic microenvironment of microcalcifications during formation and growth. Lattice parameters have previously been measured in breast microcalcifications within histological sections using SR (ref). We show here for the first time that lattice parameters be measured in this type of specimen using laboratory equipment. Furthermore, previous work [14] has determined that the mean lattice parameters of apatite calcifications within benign and malignant breast lesions differ by 0.14% and 0.15% for ‘a’ and ‘c’ respectively (ref). This study has demonstrated that these lattice parameters can be measured with a laboratory diffractometer to within 0.05%, and are thus of sufficient precision to be clinically relevant. The differences between lattice parameter values measured using SR and laboratory sources are perhaps to be expected given that one measurement is a volumetric subset of the other; the ST and laboratory measurement volumes were ~250 μm^3 and 5000 μm^3 respectively. However, determining the absolute values for these parameters was not critical here as this work has focused upon the precision with which the parameters can be measured in the laboratory.

The use of laboratory equipment for measuring phase composition and crystallographic parameters has important advantages for future studies of the chemistry of pathological calcifications. There is a growing consensus about the necessity for new biomarker tests to better identify cancer types in patients and aid in selecting suitable treatments [16]. Pathological calcification is a common feature in many cancers, and understanding calcification chemistry is increasingly seen as a biomarker for predicting disease progression [9]. The use of laboratory systems allows on-demand measurement within tissue sections which have been processed and cut using standard histological methods. This offers an efficient route to identifying new biomarkers. It also supports the development of models to understand tissue changes at the onset of malignancy, test hypotheses such as microenvironment immortalization, and create predictive tools to differentiate between indolent and aggressive cancers. However, it would be somewhat remiss if we did not consider

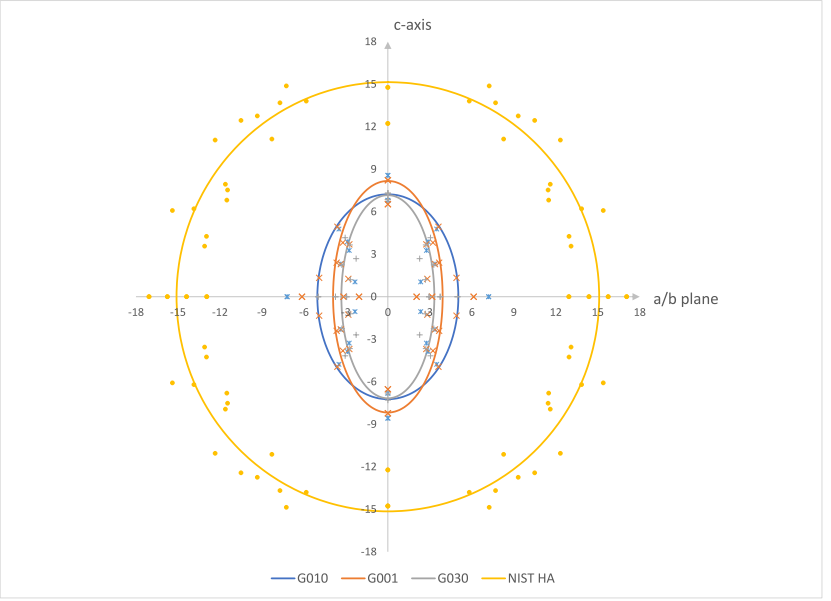

Fig. 4. The apatite calcification anisotropy illustrated in a polar plot of domain size. Each data point represents the thickness of the coherently diffracting domains in the crystallographic direction corresponding each peak. For comparison, the plot also shows data from a hydroxyapatite standard comprised of isotropic crystallites with a high degree of structural order.

the rather extended laboratory data collection time compared to the corresponding SR acquisitions. This was the result of using a conventional, fixed anode X-ray source. Recent developments (e.g. the Excillium, 'liquid-metal-jet') have led to commercial sources with significantly increased brightness (100x – 1000x) [17,18] compared to the source we used, thus enabling laboratory measurement times in seconds. We therefore hope to extend this initial study further by exploiting such state-of-the-art laboratory sources that are thus capable of significantly reducing data acquisition times for each calcification.

Competing or conflicting interests

None of the authors have any competing or conflicting interests regarding this work.

Data availability

Data will be made available on request from the corresponding author.

CRediT authorship contribution statement

Iain D. Lyburn: Writing – original draft, Methodology. **Robert Scott:** Validation, Methodology, Formal analysis. **Eleanor Cornford:** Writing – original draft, Resources. **Pascaline Bouzy:** Writing – review & editing, Investigation, Formal analysis. **Nicholas Stone:** Writing – review & editing, Investigation, Funding acquisition. **Charlene Greenwood:** Writing – review & editing, Validation, Investigation. **Ihsanne Bouybayoune:** Validation, Methodology, Investigation. **Sarah E. Pinder:** Writing – review & editing, Funding acquisition, Conceptualization. **Keith Rogers:** Writing – original draft, Supervision, Project administration, Funding acquisition, Data curation, Conceptualization.

Declaration of competing interest

The other authors, they declare that they have no known competing financial interests or personal relationships that could have appeared to influence the work reported in this paper.

Acknowledgements

This work was supported by a Medical Research Council research grant [MR/T000406/1] that funded the conduct of the research and preparation of the article. We would like to thank Andrew Usher and Monika Blaszczyk of the Department of Pathology, Cheltenham General Hospital for sectioning the tissue samples used in this study. We are grateful to Mrs. Hilary Stobart of Independent Cancer Patients' Voice (ICPV) for acting as patient representative and to all the donors who provided tissue for this study.

References

[1] T. Tot, M. Gere, S. Hofmeyer, A. Bauer, U. Pellas, The clinical value of detecting microcalcifications on a mammogram, Semin. Cancer Biol. 301 (2019) 127065, https://doi.org/10.1016/j.semcancer.2019.10.024.

[2] Y.S. Leong, K. Hasikin, K.W. Lai, N. Mohd Zain, M.M. Azizan, Microcalcification Discrimination in Mammography using Deep Convolutional Neural network: towards rapid and early breast cancer diagnosis, Front. Public Heal. 10 (2022), https://doi.org/10.3389/fpubh.2022.875305.

[3] R. Hou, L.J. Grimm, M.A. Mazurowski, J.R. Marks, L.M. King, C.C. Maley, T. Lynch, M. van Oirsouw, K. Rogers, N. Stone, M. Wallis, J. Teuwen, J. Wesseling, E. S. Hwang, J.Y. Lo, Prediction of upstaging in Ductal Carcinoma in situ based on mammographic radiomic features, Radiology (2022), https://doi.org/10.1148/radiol.210407.

[4] N. Vidavsky, J.A.M.R. Kunitake, L.A. Estroff, Multiple pathways for pathological calcification in the human body, Adv. Healthc. Mater. 10 (2021), https://doi.org/10.1002/adhm.202001271.

[5] A. Rizwan, S.K. Paidi, C. Zheng, M. Cheng, I. Barman, K. Glunde, Mapping the genetic basis of breast microcalcifications and their role in metastasis, Sci. Rep. 8 (2018) 11067, https://doi.org/10.1038/s41598-018-29330-9.

[6] P. Bouzy, S. O'Grady, H. Madupalli, M. Tecklenburg, K. Rogers, F. Palombo, M.P. Morgan, N. Stone, A time-course Raman spectroscopic analysis of spontaneous in vitro microcalcifications in a breast cancer cell line, Lab. Investig. 101 (2021) 1267–1280, https://doi.org/10.1038/s41374-021-00619-0.

[7] J.A.M.R. Kunitake, D. Sudilovsky, L.M. Johnson, H.-C. Loh, S. Choi, P.G. Morris, M.S. Jochelson, N.M. Iyengar, M. Morrow, A. Masic, C. Fischbach, L.A. Estroff, Biomineralogical signatures of breast microcalcifications, Sci. Adv. 9 (2023), https://doi.org/10.1126/sciadv.ade3152.

[8] Y. Zhang, C. Wang, Y. Li, A. Lu, F. Meng, F. Mei, J. Liu, K. Li, C. Yang, J. Du, Y. Li, Carbonate and cation substitution in hydroxylapatite in breast cancer microcalcifications, Mineral. Mag. (2021) 1–40, https://doi.org/10.1180/mgm.2021.23.

[9] S.B. Gosling, E.L. Arnold, S.K. Davies, H. Cross, I. Bouybayoune, D. Calabrese, J. Nallala, S.E. Pinder, L. Fu, E.H. Lips, L. King, J. Marks, A. Hall, L.J. Grimm, T. Lynch, D. Pinto, H. Stobart, E.S. Hwang, J. Wesseling, K. Geraki, N. Stone, I.D. Lyburn, C. Greenwood, K.D. Rogers, A. Thompson, S. Nik-Zainal, E.J. Sawyer, H. Davies, A. Futreal, N. Navin, J. Jonkers, J. van Rheenen, F. Behbod, M. Schmidt, L.F.A. Wessels, D. Rea, P. Bhattacharjee, D. Collyar, E. Verschuur, M. van Oirsouw, Microcalcification crystallography as a potential marker of DCIS recurrence, Sci. Rep. 13 (2023) 1–10, https://doi.org/10.1038/s41598-023-33547-8.

[10] R. Baker, K.D. Rogers, N. Shepherd, N. Stone, New relationships between breast microcalcifications and cancer, Br. J. Cancer 103 (2010) 1034–1039, https://doi.org/10.1038/sj.bjc.6605873.

[11] F.A. Shah, Magnesium whitlockite – omnipresent in pathological mineralisation of soft tissues but not a significant inorganic constituent of bone, Acta Biomater. 125 (2021) 72–82, https://doi.org/10.1016/j.actbio.2021.02.021.

[12] A.A. Coelho, Indexing of powder diffraction patterns by iterative use of singular value decomposition, J. Appl. Crystallogr. 36 (2003) 86–95, https://doi.org/10.1107/S0021889802019878.

[13] J.I. Langford, A. Boultif, J.P. Auffrédic, D. Louër, The use of pattern decomposition to study the combined X-ray diffraction effects of crystallite size and stacking faults in ex-oxalate zinc oxide, J. Appl. Crystallogr. 26 (1993) 22–33, https://doi.org/10.1107/S0021889892007684.

[14] R. Scott, N. Stone, C. Kendall, K. Geraki, K. Rogers, Relationships between pathology and crystal structure in breast calcifications: an in situ X-ray diffraction study in histological sections, Npj Breast Cancer 2 (2016) 16029, https://doi.org/10.1038/npjbcancer.2016.29.

[15] L. Frappart, M. Boudeulle, J. Boumendil, H.C. Lin, I. Martinon, C. Palayer, Y. Mallet-Guy, D. Raudrant, A. Bremond, Y. Rochet, J. Feroldi, Structure and composition of microcalcifications in benign and malignant lesions of the breast: study by light microscopy, transmission and scanning electron microscopy, microprobe analysis, and X-ray diffraction, Hum. Pathol. 15 (1984) 880–889, https://doi.org/10.1016/S0046-8177(84)80150-1.

[16] K. Helin, Use of Biomarkers in Cancer Research and Treatment, 2022. https://www.icr.ac.uk/about-us/policy-and-engagement/use-of-biomarkers-in-cancer-research-and-treatment.

[17] M. Wansleben, C. Zech, C. Streeck, J. Weser, C. Genzel, B. Beckhoff, R. Mainz, Photon flux determination of a liquid-metal jet X-ray source by means of photon scattering, J. Anal. At. Spectrom. 34 (2019) 1497–1502, https://doi.org/10.1039/C9JA00127A.

[18] R. Behling, Modern Diagnostic X-Ray Sources Technology, Manufacturing, Reliability, second ed., CRC Press, Boca Raton, 2021 https://doi.org/10.1201/9781003095408.